

This work has been submitted to the IEEE for possible publication. Copyright may be transferred without notice, after which this version may no longer be accessible.

Personal Dosimetry in Pulsed Photon Fields with the Dosepix Detector

Dennis Haag^{1,*}, Sebastian Schmidt¹, Patrick Hufschmidt¹, Gisela Anton¹, Rafael Ballabriga³, Rolf Behrens², Michael Campbell³, Franziska Eberle¹, Christian Fuhg², Oliver Hupe², Xavier Llopert³, Jürgen Roth², Lukas Tlustos³, Winnie Wong⁴, Hayo Zutz², and Thilo Michel¹

¹ Erlangen Centre for Astroparticle Physics, Friedrich-Alexander Universität Erlangen-Nürnberg, 91058 Erlangen, Germany

² Physikalisch-Technische Bundesanstalt (PTB), 38116 Braunschweig, Germany

³ CERN, 1211 Geneva, Switzerland

⁴ was with CERN, 1211 Geneva, Switzerland. She is now with Mercury Systems, 1212 Geneva, Switzerland

* E-mail: dennis.den.haag@fau.de

Abstract

First investigations regarding dosimetric properties of the hybrid, pixelated, photon-counting Dosepix detector in a pulsed photon field (RQR8) for the personal dose equivalent $H_p(10)$ are presented. The influence quantities such as pulse duration and dose rate were varied, and their responses were compared to the legal limits provided in PTB-A 23.2. The variation of pulse duration at a nearly constant dose rate of 3.7 Sv/h shows a flat response around 1.0 from 3.6 s down to 2 ms. A response close to 1.0 is achieved for dose rates from 0.07 mSv/h to 35 Sv/h for both pixel sizes. Above this dose rate, the large pixels (220 μm edge length) are below the lower limit. The small pixels (55 μm edge length) stay within limits up to 704 Sv/h. The count rate linearity is compared to previous results, confirming the saturating count rate for high dose rates.

Index Terms— Pulsed photon fields, hybrid pixel detector, active personal dosimetry

1 Introduction

Dosimetry in pulsed photon fields with active electronic personal dosimeters (APDs) is an important topic of the last decade. A pulsed radiation field is defined as ionizing radiation with a pulse duration shorter than 10 s [1]. With this definition, most X-ray tubes in medical applications are classified as pulsed radiation emitters [2]. Tests performed in [3–6] showed an insufficient response of APDs in pulsed photon fields, with the main issue being high peak pulse dose rates and short radiation pulse durations. The EURADOS Report 2012-02 [7] confirmed these findings with only a hybrid dosimeter being able to determine the dose within $\pm 30\%$ at high dose rates up to 55 Sv/h. This can be an issue, especially in interventional radiology and interventional cardiology (IR/IC), where staff would profit from an APD with the capability to detect low energies and pulsed radiation [7]. It was further found that APDs are almost entirely insensitive in the direct beam of medical diagnostic situations where a pulse duration smaller than 20 ms and a dose rate up to 400 Sv/h can be expected [4]. The Dosepix detector [8] was developed in order to circumvent such problems. In this work, the dose rate and pulse duration dependence of the normalized response for the personal dose equivalent $H_p(10)$ were measured in a pulsed photon field with the Dosepix detector on an ISO (International Organization for Standardization) water slab phantom in accordance with ISO standards [9, 10]. In the following, the corresponding results are presented.

2 The Dosepix detector

Dosepix is a hybrid, pixelated, photon-counting X-ray detector. The hybrid design consists of an application-specific integrated circuit (ASIC) and a semiconductor sensor layer connected pixelwise to the ASIC. As described in [11] and in this work, a 300 μm thick silicon sensor is used. The pixel layout comprises 16 \times 16 square pixels with 220 μm pixel pitch with a p-in-n doping profile. The upper two and lower two rows of the pixel matrix consist of small pixels

with an edge length of 55 μm , while the remaining 12 rows consist of larger pixels with an edge length of 220 μm . The smaller pixels detect fewer events than the larger pixels and therefore have a lower tendency for pile-up, which allows applications at high-flux conditions. The Dosepix can be operated in 3 different programmable modes: the photon-counting mode, the integration mode, and the energy-binning mode. Here, the Dosepix detector is used in the latter one, which is used for dosimetry applications. The energy-binning mode pixelwise counts events in one of 16 histogram bins according to the deposited energy of the event. The energy bin edges are individually programmed for each pixel. The Dosepix operates dead-time-free using the rolling-shutter principle. A single column is read out at a time while the rest of the matrix continues to process signals, which is a significant advantage in practical applications in pulsed photon fields, where radiation pulses are random in time. Information regarding the characterizations of Dosepix with X-rays and analog test-pulses can be found in [12], and measurements of the count rate linearity in dependence of the dose rate can be found in [13]. A dosimetry system consisting of 3 Dosepix detectors is utilized as described in [11], where the energy and angular dependence in continuous photon fields were already presented.

3 Methods

The tests in pulsed photon fields were performed in collaboration with and at the PTB (Physikalisch-Technische Bundesanstalt Braunschweig) using its X-ray unit for pulsed radiation GESA (GEpulste Strahlungs Anlage) presented in [4]. The chosen reference radiation field is the medical radiation quality RQR8 with a tube voltage of 100 kV filtered with 3.36 mm aluminum and a mean energy (fluence) of 51 keV [14]. Each measurement was repeated 2 or 3 times for statistical purposes. According to ISO standards [10], the dosimeter was irradiated on an ISO water slab phantom. However, to achieve very high dose rates up to 1080 Sv/h, the dosimeter had to be irradiated relatively close to the X-ray tube resulting in small field diameters down to 8.5 cm. In these cases the dosimetry system was irradiated without the ISO water slab phantom which has a 30 cm \times 30 cm cross-section. Correction factors were determined for measurements with and without the phantom and measurements with a small (8.5 cm) and a large (42.0 cm) field diameter. The correction factors are stated in Table 1 and were used to correct all measurements to the equivalent of the dosimetry system being placed on the ISO water slab phantom that is completely irradiated to guarantee $H_p(10)$ conditions. The quantity of interest is the change of the response R relative to the response at reference conditions R_0 , i.e., the normalized response. The response is defined by the ratio of the indication (calculated dose with Dosepix) and the reference dose determined by monitor ionization chambers which are practically independent of the dose rate and pulse duration. The change of the normalized response has to fulfill the following condition according to [15]

$$1 + f_{\min} \leq R_{\text{Norm}}^i = \frac{R_i}{R_0} = \frac{H_{\text{DPX}}^i H_{\text{ref}}^0}{H_{\text{ref}}^i H_{\text{DPX}}^0} \leq 1 + f_{\max} \quad (1)$$

with R_i being the response at measurement i , H_{DPX} the dose measured by the Dosepix dosimetry system, H_{ref} the reference dose, and f_{\min} and f_{\max} depending on the influence quantity (see Table 2). The statistical uncertainty of the normalized response is calculated via:

$$u(R_{\text{Norm}}^i) = R_{\text{Norm}}^i \sqrt{\left(\frac{u(H_{\text{DPX}}^i)}{H_{\text{DPX}}^i} \right)^2 + \left(\frac{u(H_{\text{ref}}^i)}{H_{\text{ref}}^i} \right)^2}. \quad (2)$$

The minimum requirements for the dose rate and pulse duration for conformity assessment are shown in Table 2.

Table 1: Correction factors for the phantom influence and the field-diameter influence

Pixel size	Presence of Phantom correction	Field diameter correction
55 μm	1.148 \pm 0.004	1.033 \pm 0.003
220 μm	1.168 \pm 0.002	1.024 \pm 0.007

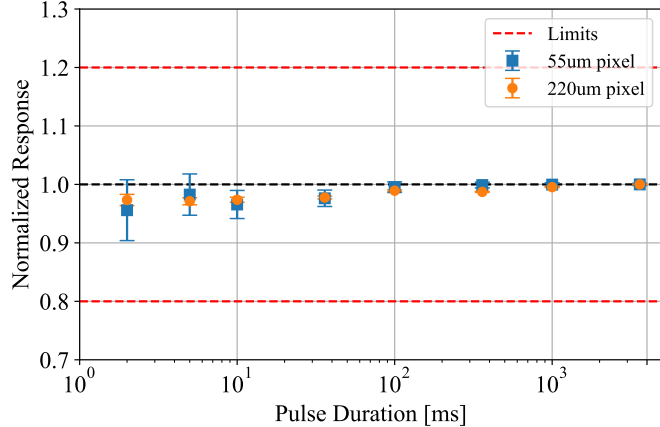


Figure 1: Normalized response for $H_p(10)$ in an RQR8 photon reference field. Influence quantity is the pulse duration at nearly constant dose rate. The uncertainty bars are calculated via (2).

4 Results and Discussion

4.1 Dependence on the pulse duration

The pulse duration was varied between 2 ms and 3.6 s, while the dose rate was held nearly constant at 3.7 Sv/h. Due to the dead-time-free measurement of the Dosepix, no dependency on pulse duration is expected. Figure 1 shows the normalized response for both pixel sizes. The response value at 3.6 s was chosen as reference R_0 . The normalized response is flat within the margin of the uncertainty bars. Overall, all data points are within limits.

4.2 Dependence on the dose rate

The measurements for the dependence on the dose rate were performed in the range from 0.07 mSv/h to 1080 Sv/h. To achieve such dose rates, both the reference dose and the pulse duration were varied. The response for both the small and large pixels was evaluated and is shown in Figure 2. Both pixel sizes have a nearly flat response up to about 35 Sv/h. The normalized response of the large pixels falls under the lower limit, slightly below 100 Sv/h, whereas for the small pixels, a dose rate up to about 704 Sv/h is achievable in the used reference field. The small pixels would allow an active warning in accident situations, e.g., if the person is exposed to the direct X-ray beam of a medical diagnostic X-ray tube where dose rates up to 400 Sv/h can occur [4].

Table 2: Minimum requirements for conformity assessment according to PTB-A 23.2 [15] for $H_p(10)$ dosimeters

Quantity	Minimum rated range of use	Reference value	f_{\min}, f_{\max}
Dose rate	0.1 μ Sv/h to 1 Sv/h	1 mSv/h	-0.13, 0.18
Radiation pulse duration	1 ms to 10 s	Response at continuous radiation	-0.2, 0.2

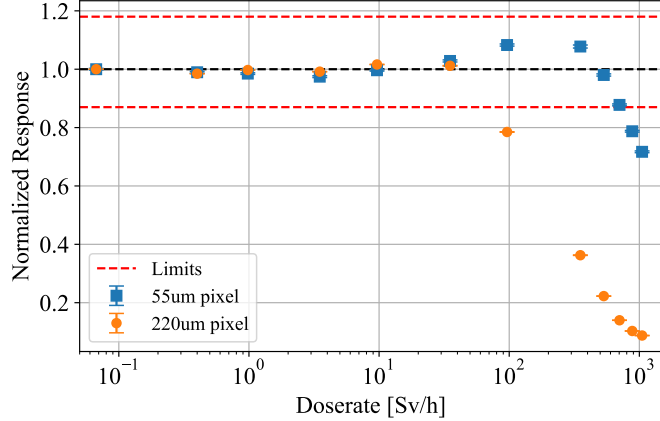


Figure 2: Normalized response for $H_p(10)$ in an RQR8 photon reference field. Influence quantity is the dose rate. The uncertainty bars are calculated via (2).

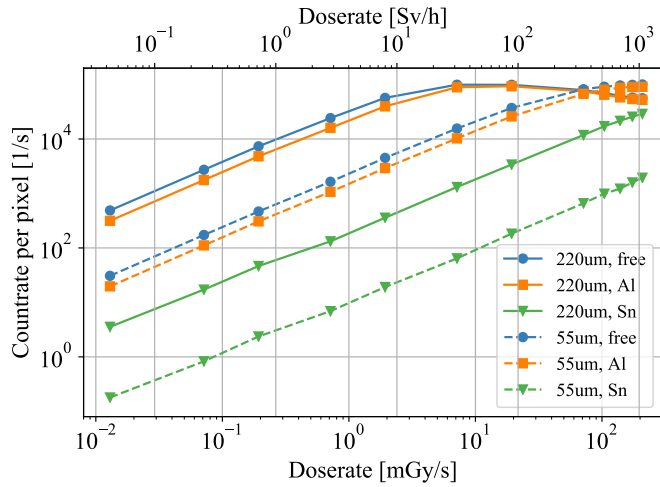


Figure 3: Count rate linearity in an RQR8 photon reference field. Influence quantity is the dose rate. The individual count rates of the three differently filtered detectors and their different pixel sizes are shown.

4.3 Count rate linearity

The measurements with the RQR8 spectrum when varying the dose rate are compared to previous measurements performed in [13]. For comparability, the abscissa is first re-scaled to Sv/s and then divided by the $H_p(10)/K_{\text{air}}$ conversion coefficient for the RQR8 spectrum (1.438 Sv/Gy). The results are shown in Figure 3 for each pixel size of the three detectors and are additionally labeled by their filter cap, i.e., aluminum cylinder with a thin aluminum foil on its top, which has a hole above the sensor (free), aluminum half-sphere (Al), and tin half-sphere (Sn). Similar behavior is observed as presented by Zang et al. [13], which means that the count rate saturates with high dose rates for unfiltered or weakly filtered detectors. The Dosepix filtered with tin shows for both pixel types no saturation and overall a low count rate. The explanation for the saturation is stated by Zang et al. in arguing that analog pile-up is increasing with an increasing dose rate which is equal to an increase of the flux. Therefore, an increase in the dose rate flattens the deposition spectrum in the detector, namely by converting several low-energy photons into a single high-energy event. For dosimetry, this implies that the dose determination is impacted. A correlation between the normalized response and count rate is observed. From the turning point at 35 Sv/h onward, the response falls below the limit. The compensation of the larger values of the conversion factor in higher energy bins is not strong enough to counteract the loss of separate events. Even due to the count rate saturation and analog pile-up, a good normalized response is achieved. The reason for this is that one of the three detectors - namely the Dosepix filtered with the tin

cap - is only in the beginning stage of its saturation. The latter statement implies that its 16 energy bins appropriately represent the energy deposition spectrum and that its partial dose is still correctly determined.

5 Conclusion

The Dosepix detector's dependence of the normalized response in an RQR8 pulsed photon field (with a mean energy of 51 keV) was shown for the variation of the pulse duration and the variation of the dose rate. Both tests show promising results for applying the Dosepix detector as an active personal dosimeter in pulsed photon fields. Further tests in different energy ranges need to be performed to identify the largest possible dose rate within the legal limits for the normalized response. The pulse duration independence of the dose measured by the prototype of a Dosepix dosimetry system is a direct result of the dead-time-free readout principle of the Dosepix acting as a camera-like radiation detector. Even the shortest pulse durations will not pose any problems to the Dosepix detector, provided that the dose rate during the pulse does not exceed certain limits. As demonstrated here, these limits concerning dose rate are substantial - i.e., in the order of 100 Sv/h and higher - compared to other commercial electronic dosimeters that saturate in the region of a few Sievert per hour. Therefore, it is concluded that the Dosepix detector is a viable detector for dosimetry of pulsed photon fields.

Acknowledgements

This project is funded by the Deutsche Forschungsgemeinschaft (DFG, German Research Foundation) - 394324524.

References

- [1] ISO, "Radiological protection - Characteristics of reference pulsed radiation - Part 1: Photon radiation," *ISO/TS 18090-1:2015*.
- [2] U. Ankerhold, O. Hupe, and P. Ambrosi, "Deficiencies of active electronic radiation protection dosimeters in pulsed fields," in *Radiation Protection Dosimetry*, vol. 135, no. 3, pp. 149–153, Jul. 2009, doi:10.1093/rpd/ncp099.
- [3] I. Clairand, J.-M. Bordy, J. Daures, J. Debroas, M. Denoziere, L. Donadille, M. Ginjaume, C. Itie, C. Koukorava, S. Krim, A.-L. Lebacq, P. Martin, L. Struelens, M. Sans-Merce, M. Tasic, and F. Vanhavere, "Active personal dosimeters in interventional radiology: tests in laboratory conditions and in hospitals," in *Radiation Protection Dosimetry*, vol. 144, no. 1-4, pp. 453–458, Mar. 2011, doi:10.1093/rpd/ncq556.
- [4] O. Hupe, H. Zutz, and J. Klammer, "Radiation protection dosimetry in pulsed radiation fields," presented at IRPA 13 Glasgow. [Online]. Available: "<https://www.irpa.net/members/TS2f.3.pdf>".
- [5] O. Hupe, S. Friedrich, F. Vanhavere, and M. Brodecki, "Determining the dose rate dependence of different active personal dosimeters in standardized pulsed and continuous radiation fields," in *Radiation Protection Dosimetry*, vol. 187, no. 3, pp. 345–352, Sep. 2019, doi:10.1093/rpd/ncz173.
- [6] F. Vanhavere, E. Carinou, I. Clairand, O. Ciraj-Bjelac, F. De Monte, J. Domienik-Andrzejewska, P. Ferrari, M. Ginjaume, H. Hršak, O. Hupe, Z. Knezevic, U. O'Connor, M. S. Merce, S. Sarmento, A. Savary, and T. Siskoonen, "The use of active personal dosimeters in interventional workplaces in hospitals: comparison between active and passive dosimeters worn simultaneously by medical staff," in *Radiation Protection Dosimetry*, vol. 188, no. 1, pp. 22–29, Dec. 2019, doi:10.1093/rpd/ncz253.
- [7] European Radiation Dosimetry Group e. V., "EURADOS Report 2012-02. ORAMED: Optimization of radiation protection of medical staff," Braunschweig, Apr. 2012.
- [8] W. Wong, G. Anton, R. Ballabriga, M. Böhnel, M. Campbell, E. Heijne, X. Llopert, T. Michel, I. Münster, R. Plackett, P. Sievers, P. Takoukam, L. Tlustos, and P. Valerio, "A pixel detector asic for dosimetry using time-over-threshold energy measurements," in *Radiation Measurements*, vol. 46, no. 12, pp. 1619–1623, Dec. 2011, doi:10.1016/j.radmeas.2011.06.061.
- [9] ISO, "Radiological protection - X and gamma reference radiation for calibrating dosimeters and doserate meters and for determining their response as a function of photon energy — Part 1: Radiation characteristics and production methods," *ISO 4037-1:2019*.
- [10] ISO, "Radiological protection - X and gamma reference radiation for calibrating dosimeters and doserate meters and for determining their response as a function of photon energy — Part 3: Calibration of area and personal dosimeters and the measurement of their response as a function of energy and angle of incidence," *ISO 4037-3:2019*.

- [11] D. Haag, S. Schmidt, P. Hufschmidt, F. Eberle, T. Michel, G. Anton, O. Hupe, J. Roth, C. Fuhg, H. Zutz, R. Behrens, M. Campbell, X. Llopart, R. Ballabriga, L. Tlustos, and W. Wong, "Personal dosimetry in continuous photon radiation fields with the dosepix detector," in *IEEE Transactions on Nuclear Science*, vol. 68, no. 5, pp. 1129–1134, May 2021, doi:10.1109/TNS.2021.3068832.
- [12] I. Ritter, G. Anton, R. B. Sune, F. Bisello, M. Campbell, T. Gabor, X. L. Cudie, S. Wölfel, W. S. Wong, and T. Michel, "Characterization of the dosepix detector with xrf and analog testpulses," in *Journal of Instrumentation*, vol. 9, no. 05, p. C05069, May 2014, doi:10.1088/1748-0221/9/05/C05069.
- [13] A. Zang, G. Anton, R. Ballabriga, F. Bisello, M. Campbell, J. Celi, A. Fauler, M. Fiederle, M. Jensch, N. Kochanski, X. Llopart, N. Michel, U. Mollenhauer, I. Ritter, F. Tennert, S. Wölfel, W. Wong, and T. Michel, "The dosepix detector—an energy-resolving photon-counting pixel detector for spectrometric measurements," in *Journal of Instrumentation*, vol. 10, no. 04, p. C04015, Apr. 2015, doi:10.1088/1748-0221/10/04/C04015.
- [14] IEC, "Medical diagnostic X-ray equipment - Radiation conditions for use in the determination of characteristics," *IEC 61267:2005*.
- [15] Physikalisch-Technische Bundesanstalt (PTB), "PTB-Anforderungen PTB-A 23.2: Strahlenschutzmessgeräte; Personendosimeter zur Messung der Tiefen- und Oberflächen-Personendosis. Ausgabe November 2013," doi:10.7795/510.20151109M.